

## Spectroscopy of Nitrophenolates in Vacuo: Effect of Spacer, Configuration, and Microsolvation on the Charge-Transfer Excitation Energy

Steen Brøndsted Nielsen,<sup>\*,†</sup> Mogens Brøndsted Nielsen,<sup>\*,‡</sup> and Angel Rubio<sup>\*,§</sup>

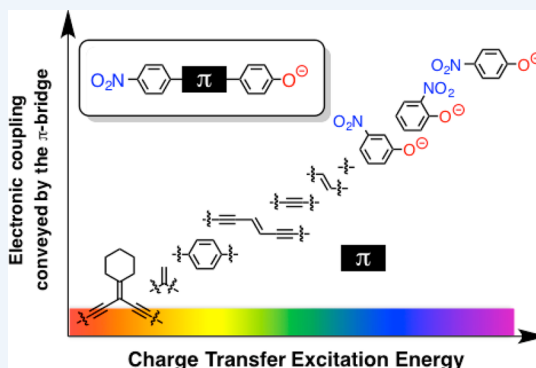
<sup>†</sup>Department of Physics and Astronomy, Aarhus University, Ny Munkegade 120, DK-8000 Aarhus C, Denmark

<sup>‡</sup>Department of Chemistry & Center for Exploitation of Solar Energy, University of Copenhagen, Universitetsparken 5, DK-2100 Copenhagen Ø, Denmark

<sup>§</sup>NanoBio Spectroscopy Group and ETSF Centre for Scientific Development, Centro Mixto CSICUPV/EHU "Física de Materiales", University of the Basque Country UPV/EHU Centro Joxe Mari Korta, Avenida de Tolosa, 72, E-20018 Donostia-San Sebastian, Spain

**CONSPECTUS:** In a charge-transfer (CT) transition, electron density moves from one end of the molecule (donor) to the other end (acceptor). This type of transition is of paramount importance in nature, for example, in photosynthesis, and it governs the excitation of several protein biochromophores and luminophores such as the oxyluciferin anion that accounts for light emission from fireflies. Both transition energy and oscillator strength are linked to the coupling between the donor and acceptor groups: The weaker the coupling, the smaller the excitation energy. But a weak coupling necessarily also causes a low oscillator strength possibly preventing direct excitation (basically zero probability in the noncoupling case). The coupling is determined by the actual spacer between the two groups, and whether the spacer acts as an insulator or a conductor. However, it can be difficult or even impossible to distinguish the effect of the spacer from that of local solvent molecules that often cause large solvent shifts due to different ground-state and excited-state stabilization. This calls for gas-phase spectroscopy experiments where absorption by the isolated molecule is identified to unequivocally establish the intrinsic molecular properties with no perturbations from a microenvironment. From such insight, the effect of a protein microenvironment on the CT excited state can be deduced.

In this Account, we review our results over the last 5 years from mass spectroscopy experiments using specially designed apparatus on several charged donor–acceptor ions that are based on the nitrophenolate moiety and  $\pi$ -extended derivatives, which are textbook examples of donor–acceptor chromophores. The phenolate oxygen is the donor, and the nitro group is the acceptor. The choice of this system is also based on the fact that phenolate is a common structural motif of biochromophores and luminophores, for example, it is a constituent of the oxyluciferin anion. A presentation of the setups used for gas-phase ion spectroscopy in Aarhus is given, and we address issues of whether double bonds or triple bonds best convey electronic coupling between the phenolate oxygen and the nitro group, the significance of separating the donor and acceptor spatially, the influence of cross-conjugation versus linear conjugation, and along this line *ortho* versus *meta* versus *para* configuration, and not least the effect of a single solvent molecule (water, methanol, or acetonitrile). From systematic studies, a clear picture has emerged that has been supported by high-level calculations of electronically excited states. Our work shows that CC2 coupled-cluster calculations of vertical excitation energies are within 0.2 eV of experimental band maxima, and importantly, that the theoretical method is excellent in predicting the relative order of excitation energies of a series of nitrophenolates. Finally, we discuss future challenges such as following the change in absorption as a function of the number of solvent molecules and when gradually approaching the bulk limit.



### 1. INTRODUCTION

Some of the most important electronically excited states in nature are the charge transfer (CT) states. They form the basics of photosynthesis allowing for charge-separation processes crucial for conversion of solar energy into chemical energy.<sup>1</sup> They govern the photophysics of many protein biochromophores and bioluminophores. Examples include the thioester

derivative of the *p*-coumaric acetate chromophore located within the photoactive yellow protein (PYP),<sup>2</sup> the protonated Schiff base retinal in rhodopsin proteins involved in visual perception,<sup>3</sup> and the oxyluciferin anion within luciferase

Received: January 20, 2014

Published: March 27, 2014

responsible for light emission from fireflies.<sup>4</sup> In the latter, the molecular anion is formed in its CT state biochemically and not from light absorption that otherwise could directly or indirectly lead to it.

The degree of CT character of an electronic transition differs significantly between chromophores and is modulated by a nearby environment. The weaker the coupling between the donor and acceptor ends, the smaller is the excitation energy (Figure 1). However, in the case of no coupling (“pure” CT

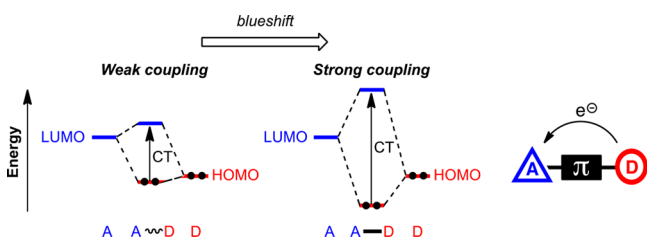


**Figure 1.** The coupling between an electron donor (where the HOMO is located) and an electron acceptor (where the LUMO is located) determines the excitation energy. (a) Weak coupling: small excitation energy. (b) Strong coupling: large excitation energy. The orbital overlap in (b) is much larger than that in (a) which implies much stronger oscillator strength in the former case.

state), the oscillator strength decreases to zero. In such situations or where coupling is weak, the CT state will not be populated directly by light absorption; it is a so-called dark state. Instead its formation proceeds via population of a higher-lying bright state that then couples to the CT state in an internal conversion (IC) process. This overall process is denoted light-induced electron transfer and should not be confused with direct CT excitation (Figure 2). In the present work, we focus on the latter.

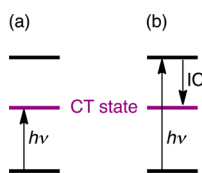


**Figure 2.** (a) Direct excitation to CT state. (b) Excitation to bright state with high oscillator strength followed by internal conversion to dark CT state. An absorption spectrum reveals the difference between the two scenarios as the excitation energies are different, though the final outcome is the same.

Many protein chromophores and luminophores possess a phenolate moiety as the donor group and various acceptor groups. To model the physics of such systems, we studied nitrophenolate anions (Figure 3). In all these ions, the phenolate oxygen is the donor and the nitro group is the acceptor. However, as discussed in the following, the degree of coupling differs significantly between them, which is revealed as differences in absorption band maxima. It is the spacer between the two groups that controls the electronic coupling and as a result determines the transition energy and oscillator strength. The spacer can be thought of as the molecular analogue of a resistor between the donor and acceptor. In the *meta*-isomer **1**, the two groups are cross-conjugated relative to each other, while they are linearly conjugated in *ortho*- and *para*-isomers **2** and **3**. A cross-conjugated pathway between two groups involves two consecutive single bonds; that is, a double bond will branch

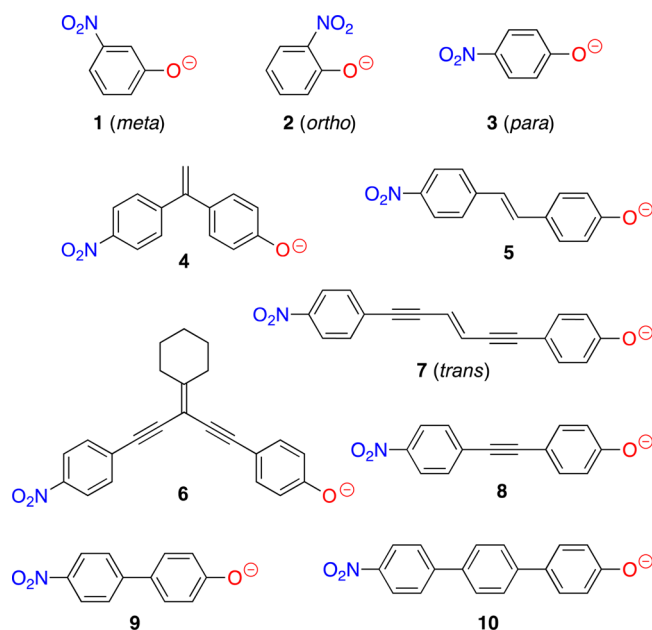


**Figure 3.** Nitrophenolate subjects of study.

off along the path being traversed (Figure 4). Influence of cross-conjugation versus linear conjugation in extended nitro-

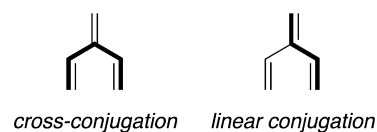


**Figure 4.** Conjugation pathways in 3-methylidene-1,4-pentadiene.

phenolates is also revealed by comparing properties of the ethylene-bridged chromophores **4** and **5** and the diethynylene-bridged chromophores **6** and **7**. Comparison of the stilbene derivative **5** and the tolane derivative **8** sheds light on the difference between an alkene and alkyne spacer. Finally, in the progression **3**–**9**–**10**, the donor and acceptor are separated by an increasing number of phenylene units, which allows for elucidating the distance dependence and decoupling by deviations from planarity (*ortho* H<sub>2</sub>H clash in biphenyls).

To fully comprehend the photophysics of these ions, it is important to study them free of an environment, as nearby solvent molecules may perturb the electronic structure in nonobvious ways. One approach is to characterize the chromophores spectroscopically in solvents of decreasing polarity and thereafter extrapolate to vacuum. Several solvent polarity scales exist based on the energy of inter- or intramolecular CT transitions, such as the Dimroth–Reichardt E<sub>T</sub>(30),<sup>5</sup> the Z-scale,<sup>6</sup> the π\*-scale,<sup>7</sup> and scales taking into account H-bond interactions.<sup>8</sup> The situation is more difficult when the aim is to correlate the CT energy of charged nitrophenolates with solvent polarity. Ionophores are not easily dissolved in nonpolar solvents and even then there are field effects from counterions. Instead, we have turned to gas phase spectroscopy using specialized apparatus developed in Aarhus.

## 2. INSTRUMENTAL SETUPS FOR GAS-PHASE ION ABSORPTION SPECTROSCOPY

From a technical point of view, gas-phase spectroscopy differs in one way significantly from solution-phase spectroscopy: by

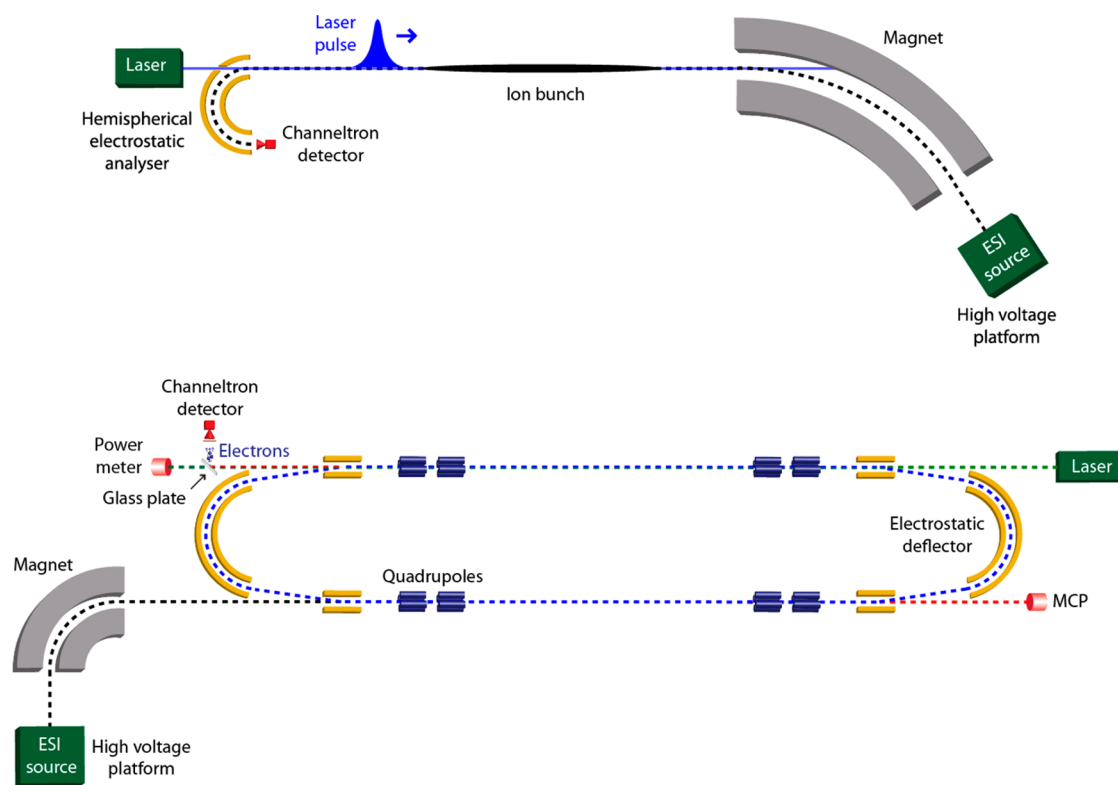


**Figure 5.** Instruments for gas-phase absorption spectroscopy. (top) Setup I: A single pass sector instrument. (bottom) Setup II: Electrostatic Ion Storage ring in Aarhus (ELISA). See text for details.

the number and number density of absorbing species present in the sample. Solutions of chromophores are colorful as they absorb visible light. It is therefore straightforward to record the decrease in light intensity versus wavelength with a conventional UV/vis spectrometer. A similar experiment on mass-selected ions isolated in vacuo is difficult, if not impossible, as the number of absorbers is too low to cause a measurable change in the light intensity. Instead, absorption is indirectly determined from the dissociation of ions after excitation. Either charged or neutral fragments are measured or/and photoelectrons for anions. This technique is coined action spectroscopy. A specialized apparatus is needed that is based on the combination of mass spectrometers and lasers.

We emphasize that there are several weaknesses as the technique relies on a number of assumptions: (1) The light emission quantum yield is assumed insignificant or constant within an absorption band. (2) Dissociation should occur on the relevant time scale of the experiment. (3) In cases where time constants for dissociation cannot be measured, either the dissociation should be complete within the window for sampling dissociation, or the rate constants should only have a weak dependence on excitation energy to reduce the role of kinetic shifts.

We have used two setups for gas-phase spectroscopy, allowing for studies on negatively charged phenolate species<sup>9–13</sup> as well as on individual donor and acceptor molecular ions.<sup>14</sup> The experiments are briefly presented in the following; for more detail we refer to refs 15 and 16. Ions are produced in gas phase by electrospray ionization and stored in a multipole ion trap. Here, either they thermalize in collisions with helium atoms, or they react with solvent molecules to form complexes. The trap is emptied at a certain repetition rate, and all ions are accelerated to high kinetic energies (keV). Ions of

interest are then selected by an electromagnet according to their mass-to-charge ratios ( $m/z$ ). This is a clean experiment in the sense that spectroscopy is performed only on ions with the right  $m/z$ , in contrast to solution-phase experiments where all absorbing species in the solution contribute to the decrease in light intensity.

The first setup (I) is a sector instrument where photofragment ions formed within microseconds after photoexcitation are mass-analyzed with an electrostatic analyzer and counted by a channeltron detector (Figure 5, top). Ions from the trap are injected into the sector field every 25 ms, and every second ion bunch is irradiated to distinguish the yield of fragment ions formed by photoexcitation from that due to unimolecular decay of metastable ions and collision-induced dissociation in the beamline. The branching ratios for the different fragmentation channels can be measured as a function of excitation wavelength.

The second setup (setup II) is a storage ring that is used to sample dissociation on longer time scales (tens of microseconds to tens of milliseconds) (Figure 5, bottom). Ions are injected in the ring and stored by its electrostatic elements. An ion circulates until it changes its  $m/z$  as a result of fragmentation. Neutrals produced on one side of the ring opposite to the side where photoexcitation is done are monitored by a microchannel plate detector (MCP) (delayed dissociation). Photoexcitation leads to an increased yield of neutral products, and from the trace of fragments the dissociation time constants are established at each wavelength within the absorption band. These are used to obtain numbers for the ions that are photoexcited by the laser pulses, on a relative and not absolute scale.<sup>17</sup> It is also possible with this setup to measure neutral products formed in the same side where photoexcitation is done to identify fast or prompt processes such as electron

detachment; the detector is here a secondary emission detector (SED) and is a channeltron that detects released electrons from a glass plate due to neutrals impact.<sup>18</sup> The ion trap is emptied every tenth of a second which is the same repetition rate as that of the laser.

For experiments at both setups, corrections are done for ion beam fluctuations based on the yield of fragments not due to photoexcitation (this number is proportional to the actual number of ions) and for the number of photons in the laser pulse.

The laser system is pumped by a Nd:YAG laser where the fundamental is frequency tripled to 355 nm. This light is injected into an optical parametric oscillator (OPO) to generate visible and infrared light (420–2300 nm). To produce light with lower wavelengths, the proper OPO output (visible or IR) is frequency doubled in a barium borate (BBO) crystal. The laser is operated at a frequency of 20 and 10 Hz in experiments at setup I and setup II, respectively.

### 3. RESULTS

#### Comparison between Experimental Absorption Band Maxima and Calculated Vertical Excitation Energies

We shall first compare our experimental and theoretical data on the nitrophenolates as summarized in Table 1. The coupled-cluster CC2 theoretical model was used for all ions and time-dependent density functional theory (TDDFT) for a selected few.

**Table 1. Experimental Band Maxima and Calculated Excitation Energies for the HOMO–LUMO Transitions<sup>a</sup>**

ion	expt	CC2	TDDFT
1 <sup>b</sup>	530 (2.34)	514 (2.41)	
1·H <sub>2</sub> O <sup>b</sup>	485 (2.56)	468 (2.65)	
1·CH <sub>3</sub> OH <sup>b</sup>	485 (2.56)	464 (2.67)	
1·CH <sub>3</sub> CN <sup>b</sup>	505 (2.46)	481 (2.58)	
2 <sup>c</sup>	399 (3.11)	412 (3.01)	
3 <sup>c</sup>	393 (3.15)	386 (3.21)	379 (3.27)
4 <sup>d</sup>		761 (1.63)	
5 <sup>e</sup>	685 (1.81)	613 (2.02)	
6 <sup>d</sup>		886 (1.40)	
7 <sup>d</sup>		736 (1.69)	
8 <sup>e</sup>	695 (1.78)	639 (1.94)	
9 <sup>f</sup>	541 (2.29)	570 (2.18)	593 (2.09)
10 <sup>f</sup>	775 (1.60)	752 (1.65)	918 (1.35)

<sup>a</sup>Values are in nm and in eV (in parentheses). <sup>b</sup>Reference 12. <sup>c</sup>Reference 11. <sup>d</sup>Reference 13. <sup>e</sup>Reference 10. <sup>f</sup>Reference 9.

First, the trend in experimental absorption band maxima is exactly the same as that predicted by CC2. Second, the correlation between experimental and CC2 values is excellent, both for bare and microsolvated ions (Figure 6). The maximum deviation is 0.2 eV or about 10% of the excitation energy, but in most cases the agreement is much better. For 4 and 6, we have not achieved experimental data (vide infra) and instead rely on the CC2 data. Fortunately, the good correlation between theory and experiment makes this approach reliable. Finally, it is evident that TDDFT performs worse than CC2 in the few cases where we have data, which is not surprising as TDDFT is known to have problems with CT excitations.<sup>19</sup> Indeed, the deviation is largest for 10 with the lowest excitation energy

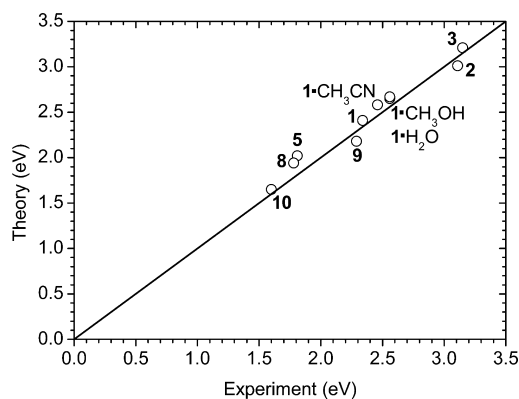


**Figure 6.** Theoretical (CC2) versus experimental results. The inserted straight line was chosen to go through the origin and to have a slope of 1.

(highest CT character). In the following, we discuss the data as a function of molecular structure.

#### *meta*-Nitrophenolate and the Effect of a Single Solvent Molecule

One of the simplest donor–acceptor systems is 1, and this ion absorbs visible light with maximum at 530 nm (2.34 eV) (Figure 7).<sup>12</sup> After photoexcitation there are four competing dissociation channels corresponding to formation of NO<sub>2</sub><sup>−</sup>, loss of CO and NO, loss of NO<sub>2</sub>, and loss of NO (Figure 8). The photoyields of each of the four fragment ions were recorded as a function of wavelength and summed to give the action spectrum shown in Figure 7. This spectrum is taken to

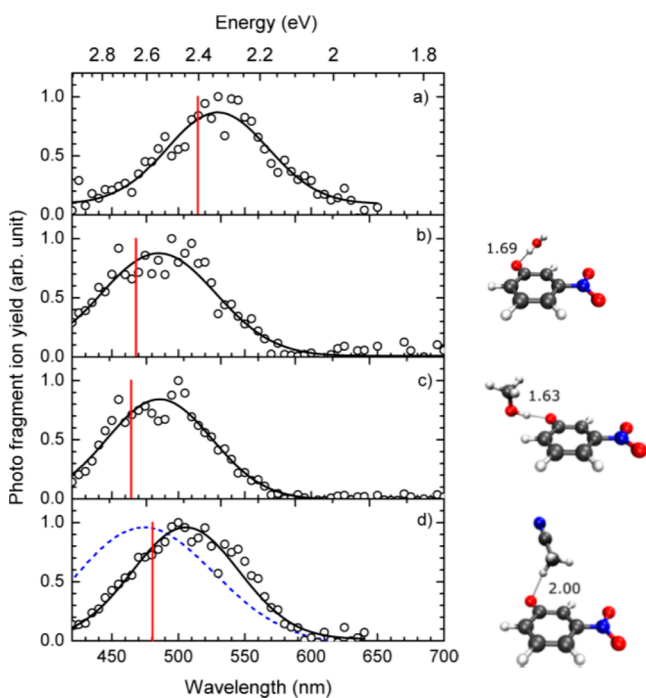


**Figure 7.** Action spectra of (a) 1 and complexes between 1 and one (b) H<sub>2</sub>O, (c) CH<sub>3</sub>OH, (d) CH<sub>3</sub>CN (setup I). The red sticks denote CC2-values. The blue dashed curve in (d) is the spectrum in acetonitrile solution. To the right, minimum-energy structures are shown calculated at the MP2 level using the TZVPP basis set (hydrogen-bond distances in Å). Reprinted with permission from ref 12. Copyright 2013 American Chemical Society.



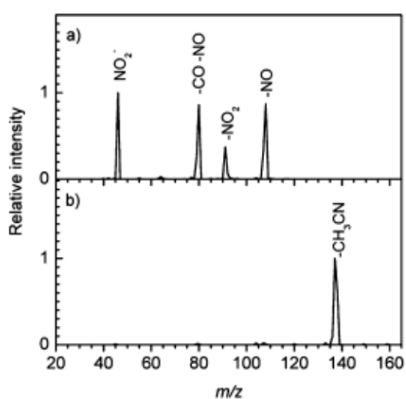


**Figure 8.** Photoinduced dissociation mass spectra of (a) **1** (510 nm light) and (b) the complex between **1** and  $\text{CH}_3\text{CN}$  (500 nm light). Reprinted with permission from ref 12. Copyright 2013 American Chemical Society.

represent the absorption spectrum of **1** in vacuo. If instead neutral products formed within the first 10  $\mu\text{s}$  after photoexcitation are measured using setup II, the band is slightly skewed toward the blue by about 0.05 eV due to electron photodetachment. The vertical detachment energy is calculated to 2.98 eV, and detachment via the electronically excited state therefore only plays a role on the blue side of the absorption band. We estimate an uncertainty in the band maximum of about 0.05 eV.

Often a chromophore is located in a hydrophobic protein pocket that provides shielding against bulk water. There is limited access to water molecules, maybe just one or two are present.<sup>20</sup> Hence it is relevant to understand the change in chromophore color by specific interactions with immobile waters or with charged or polar groups,<sup>21</sup> which is one of the most important motivations for gas-phase spectroscopy of microsolvated ions described in the following.

In the case of **1**, we found that the attachment of a single molecule, water, methanol, or acetonitrile, leads to a blue-shift of the band by 0.22, 0.22, and 0.11 eV, respectively (Figure 7).<sup>12</sup> Action spectra were recorded with setup I by sampling the loss of the solvent molecule, which is by far the dominant dissociation channel (Figure 8b). The shifts are smaller than the solvent binding energies (0.54, 0.65, and 0.50 eV for water, methanol, and acetonitrile, respectively) as expected, since there must be a favorable interaction between the ion and the molecule both in the electronic ground and excited states. Movement of electron density away from the phenolate oxygen, where the water molecule is located, toward  $\text{NO}_2$  explains the blue-shift (Figure 9) as the water binds stronger to the ion in the ground state than in the excited state. If the excitation were

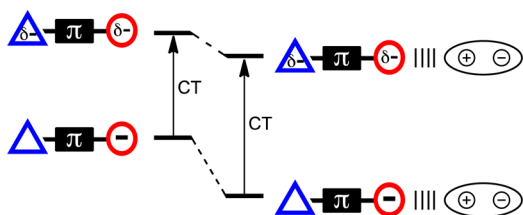


**Figure 9.** Attachment of one molecule to a bare ion lowers the ground-state energy by the binding energy. There is also a favorable interaction between the two in the CT-excited state but less so as the distance between the negative charge and the molecule is larger.

instead a localized  $\pi-\pi^*$  transition, a red-shift would be expected due to the higher polarizability in the excited state than in the ground state. It is also evident that a protic solvent molecule causes larger perturbation than a nonprotic one despite similar binding energies. The blue-shift measured for attachment of water to phenolate is similar to that earlier observed for the oxyluciferin anion (0.2 eV)<sup>22</sup> and slightly higher than that calculated for the PYP chromophore anion (0.06 eV);<sup>23</sup> both have the phenolate moiety as mentioned earlier.

In Figure 7, the absorption by **1** in bulk acetonitrile solution is also shown. The band maximum is at 2.62 eV, that is, blue-shifted by 0.28 eV.<sup>12</sup> Interestingly, a single acetonitrile molecule accounts for a significant part of the total blue-shift. In bulk water and methanol, maxima are at 3.18 and 3.20 eV. Hence, full solvation in these two solvents results in larger shifts than in acetonitrile, which is probably linked to two or three H-bond interactions between the phenolate oxygen and water or methanol molecules thereby rendering the CT rather costly.

#### *ortho*- and *para*-Nitrophenolates

Both experiment and theory find larger excitation energies for **2** and **3** than for **1** by 0.6–0.8 eV (Table 1).<sup>11</sup> At first it seems counterintuitive that the stronger  $\pi$ -electron delocalization in these two ions (cf., resonance structures in Figure 10) results in

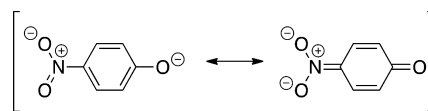


**Figure 10.** Two important resonance structures of **3**, which leads to a strong coupling of the donor and acceptor. The excess charge is delocalized over the entire ion.

higher CT energies. It is, however, important to remember that indeed larger  $\pi$ -electron delocalization lowers the excitation energy of a local  $\pi\pi^*$ . This is borne out by the decreasing HOMO–LUMO gap of conjugated oligomers as the number of monomer units increases.<sup>24</sup> But a CT is not a local excitation; it is one where the HOMO and LUMO are located at different ends of the molecule. The coupling between donor and acceptor in **2** and **3** is strong, and therefore the excitation energy is high according to the picture in Figure 1. The strong coupling in the *ortho* and *para* derivatives is in line with mesomeric effects in textbook organic chemistry: the hydroxy group is a strongly activating and *ortho-para*-directing group in electrophilic aromatic substitution of phenol, such as nitration. Experimental and quantum-chemical studies on methyl coumarates reveal similar behavior: *meta*-methyl coumarate exhibits a lower-energy CT absorption relative to the push–pull *ortho*- and *para*-isomers.<sup>25</sup>

#### Cross-Conjugation versus Linear Conjugation

*meta*-Nitrophenolate **1** presents an example of donor and acceptor ends being connected in a cross-conjugated arrangement. Thus, the two groups are not connected by alternating single and double bonds (linear conjugation) as in the *ortho*- and *para*-nitrophenolates (**2** and **3**). The geminally 1,1-disubstituted ethylene **4** is another example of a cross-conjugated molecule, while the *trans* 1,2-disubstituted ethylene **5** has donor and acceptor placed in linear conjugation. X-ray crystallographic analysis of the neutral phenol of **4** reveals that the two aryl groups are not coplanar with the central ethylene group,<sup>13</sup> causing an additional decoupling of donor and

acceptor ends. Instead, the diethynylethene-extended molecules **6** and **7** are fully planar according to calculations. The decoupling in both **4** and **6** is so significant that it was impossible to measure a CT band by solution-phase spectroscopy. Gas-phase spectroscopy was attempted for **4**, but it seems that absorption is outside the region of measurement or simply that the oscillator strength is too low. Instead, we turned to calculations: CC2 calculations reveal very low oscillator strengths for this transition in **4** (0.01) and **6** (0.06). The CT maximum of **4** was calculated to be 761 nm (1.63 eV), which is red-shifted by 0.4 eV relative to the value for **5** (613 nm, 2.02 eV). This reduced excitation energy is explained by decoupling on account of both cross-conjugation and nonplanarity (the structure of **4** is nonplanar while that of **5** is). The poor electronic communication in **4** is evident from the localized HOMO and LUMO shown in Figure 11, while the

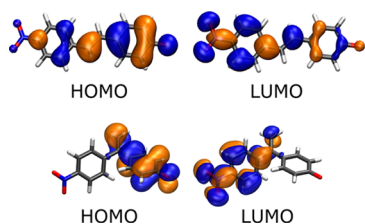


**Figure 11.** Orbitals of **4** (bottom) and **5** (top). Taken from ref 13.

orbitals of the linearly conjugated chromophore **5** are spread over both ends of the ion. Similarly, the cross-conjugated and now planar chromophore **6** exhibits a reduced excitation energy (886 nm, 1.40 eV) relative to that of the linearly conjugated **7** (736 nm, 1.69 eV). We note that inefficient electron delocalization via cross-conjugation was also established from studies on oligoenes, so-called dendralenes,<sup>26</sup> as well as from systems undergoing photoinitiated charge separation corresponding to the pathway outlined in Figure 2b.<sup>27</sup>

#### Alkene versus Alkyne Bridge

The experimental gas-phase spectrum of the toluene derivative **8** displays a maximum at 695 nm (1.78 eV), while the stilbene derivative **5** absorbs at 685 nm (1.81 eV) (Figure 12).<sup>10</sup> Similarly, CC2 calculations reveal that the absorption band maximum of **8** is red-shifted relative to that of **5** (by 0.08 eV). When comparing instead absorption properties in methanol solution of the corresponding sodium salts, it was found that **8** had a maximum (408 nm, 3.04 eV) blue-shifted relative to that of **5** (435 nm, 2.85 eV). Thus, solvation effects can mask the intrinsic effect exerted by a bridging unit, and when comparing absorption results for alkyne- and alkene-bridged donor–acceptor compounds from literature,<sup>28</sup> conflicting conclusions would be drawn with respect to which spacer conveys electronic communication most efficiently. The clear-cut result obtained by studying isolated molecules with no interfering solvent molecules, that is, an alkyne conveys the communication less efficiently than an alkene, is in accordance with molecular conductance studies on single molecules: Oligo-(phenylenevinylene)s exhibit higher conductance than oligo-(phenyleneethynylene)s.<sup>29</sup>

#### Oligo(phenylene) Bridges

Comparison of chromophores **3**, **9**, and **10** shows the effect of adding phenylene units in the spacer. Thus, concomitant red-shifts in absorption is observed when proceeding from one benzene ring (**3**, 393 nm), to a biphenyl (**9**, 541 nm), to a

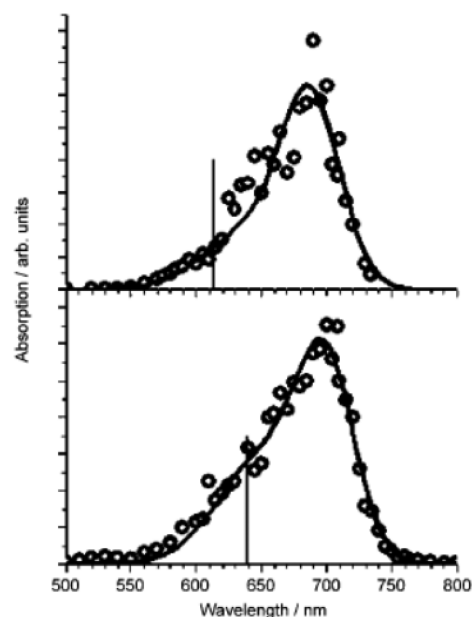


**Figure 12.** Gas-phase action spectra (setup II) and CC2-values (vertical lines) of **5** (top) and **8** (bottom). Taken from ref 10.

terphenyl (**10**, 775 nm).<sup>9</sup> These red-shifts are reasonably explained by a combination of electronic decoupling of donor and acceptor due to the nonplanar structures of **9** and **10** (as a result of *ortho*-H,H steric interactions between the aryls) and a raising of the HOMO energy and a decreasing of the LUMO energy due to extended conjugation in each end of **9** and **10**.

## 4. CONCLUSIONS AND OUTLOOK

By elucidating the intrinsic optical properties of a large selection of nitrophenolate chromophores by gas-phase action spectroscopy and quantum chemistry, it has been demonstrated clearly and in a well-controlled way that the CT excitation energy decreases with electronic decoupling between donor and acceptor as a result of either cross-conjugation or nonplanarity. This effect is not always obvious from solution-phase studies where both solvent polarity and counterion effects play a role. Knowledge on intrinsic molecular properties in the absence of interfering solvent molecules is particularly important in biochemistry and for the design of molecules for single-molecule electronics, which is a field where the concept of linear versus cross-conjugation has been recognized as a structural motif for controlling molecular conductance.<sup>30</sup>

While absorption by several bare nitrophenolates was studied in great detail, much less work has been done on microsolvated ions. It is limited to **1**, and only the effect of a single molecule was explored. As solvent molecules are gradually attached to the charged end of the chromophore, a blue-shift in the absorption is expected. However, solvation of the nitro group can lead to red-shifts as the photoactive electron moves closer to the dipoles at this end. Indeed, calculations predicted red-shifts of 0.27 and 0.25 eV for the placement of methanol and acetonitrile at the nitro group, respectively.<sup>11</sup> A smaller red-shift of 0.07 eV was reported for the PYP anion when a water was bound to the acceptor end.<sup>22</sup> The absorption should of course converge toward that in bulk solution but it is possible that on the way both blue-shifts and red-shifts are encountered. The stepwise absorption changes as a function of the number of solvent molecules are very interesting to follow. Unfortunately,

it is complicated experimentally to do this due to weak parent ion currents. However, theory has shown to describe these systems quite well, and computations are therefore a viable first approach.

Studies of microsolvation effects for other anions would also be worthwhile. Consider, for example, **2** or **3**: Is the absorption by *para*-nitrophenolate **3** with one water attached blue-shifted or red-shifted compared to the bare ion? Considering that electron density moves away from the phenolate oxygen toward NO<sub>2</sub> upon excitation, the answer is a blue-shift (see Figure 9). On the other hand, the solvent molecule localizes the charge at the phenolate oxygen in the ground-state structure and thereby makes the electronic structure more *meta*-like (the resonance formula to the right in Figure 10 diminishes in importance). If considering this decoupling of the HOMO and LUMO to be most important, the answer is a red-shift! No matter what effect is the strongest, a local solvation of **3** is expected to give a smaller overall change in absorption than that of **1** because of the two opposing effects. This raises another question: Is it possible by proper solvation of the phenolate oxygen to give **1** and **3** the same color? Finally, the *ortho* isomer **2** may behave in a third way: A water molecule can bridge the two substituents, and it is not obvious whether the resulting shift in absorption is to the blue or to the red. Experiments attacking these questions are planned by our groups.

## AUTHOR INFORMATION

### Corresponding Authors

\*E-mail: [sbn@phys.au.dk](mailto:sbn@phys.au.dk).

\*E-mail: [mbn@kiku.dk](mailto:mbn@kiku.dk).

\*E-mail: [angel.rubio@ehu.es](mailto:angel.rubio@ehu.es).

### Author Contributions

The manuscript was written through contributions of all authors. All authors have given approval to the final version of the manuscript.

### Funding

The Danish Council for Independent Research | Natural Sciences (#10-082088), the Lundbeck Foundation, and University of Copenhagen.

### Notes

The authors declare no competing financial interest.

### Biographies

**Steen Brøndsted Nielsen** received his Ph.D. in Chemistry in early 2000 from the University of Copenhagen. During his studies, he spent time at Yale, University of Oslo, and University of Alberta. He did postdoctoral work at Aarhus University (AU) and at Princeton. He has had Guest Professorships in Orsay, Caen, and Villeteuse and has since 2007 been employed as an Associate Professor in Physics at AU. His research interests lie in the fields of (bio)chromophore spectroscopy, electron-induced dissociation of biomolecular ions, molecular dianions, mass spectrometry, and synchrotron radiation circular dichroism.

**Mogens Brøndsted Nielsen** received his Ph.D. in Chemistry in 1999 from University of Southern Denmark (SDU). During his studies, he spent time at UCLA and at Université d'Angers. He did postdoctoral work at ETH in Zürich. After an Assistant Professorship at SDU, he moved in 2004 to University of Copenhagen as Associate Professor and was in 2008 promoted to Professor of organic chemistry. His research interests are rooted in organic synthesis, targeting  $\pi$ -conjugated molecules for molecular electronics and light-harvesting.

**Angel Rubio** received his Ph.D. in Physics in 1991 from the University of Valladolid (UVA), Spain. During his studies, he spent time at the Max Planck in Berlin and at Universities of Palma de Mallorca, Santader, Barcelona, Osnabruck, and Nancy. He did postdoctoral work at University of California at Berkeley. After an Associate Professorship at UVA, he moved in 2001 to University of the Basque Country as Professor/Chair of Condensed Matter Physics and Director of the Nano-Bio Spectroscopy Group. He is External Director of the Max-Planck Society and Group Director ("Theoretical Spectroscopy") of the Fritz Haber Institute of Max-Planck-Gesellschaft, Berlin. His research is rooted in theory of electronic and structural properties of condensed matter, and development of tools to investigate the electronic response of materials, nanostructures, biomolecules, and hybrid materials to electromagnetic fields.

## ACKNOWLEDGMENTS

We thank present and previous group members who have contributed to the results, in particular, Drs. M. Wanko (Universidad del País Vasco), M.-B.S. Kirketerp (AU), K. Stöckel (AU), M.Å. Petersen, M.A. Christensen (University of Copenhagen), H. Zettergren (Stockholm University), and J. Houmøller (AU).

## ABBREVIATIONS

CC2, Second-Order Approximate Coupled-Cluster; CT, charge transfer; ELISA, ELeCtrostatic Ion Storage ring in Aarhus; HOMO, highest occupied molecular orbital; IC, internal conversion; IR, infrared; LUMO, lowest unoccupied molecular orbital; MP, Møller–Plesset perturbation theory; TDDFT, time-dependent density functional theory

## REFERENCES

- (1) Berg, J. M.; Tymoczko, J. L.; Stryer, L. *Biochemistry*, 6th ed.; W.H. Freeman and Company: New York, 2007.
- (2) (a) Gromov, E. V.; Burghardt, I.; Köppel, H.; Cederbaum, L. S. Electronic structure of the PYP chromophore in its native protein environment. *J. Am. Chem. Soc.* **2007**, *129*, 6798–6806. (b) Gromov, E. V.; Burghardt, I.; Köppel, H.; Cederbaum, L. S. Native hydrogen bonding network of the photoactive yellow protein (PYP) chromophore: Impact on the electronic structure and photoinduced isomerization. *J. Photochem. Photobiol., A* **2012**, *234*, 123–134.
- (3) (a) Rajput, J.; Rahbek, D. B.; Andersen, L. H.; Hirshfeld, A.; Sheves, M.; Altoe, P.; Orlandi, G.; Garavelli, M. Probing and Modeling the Absorption of Retinal Protein Chromophores in Vacuo. *Angew. Chem., Int. Ed.* **2010**, *49*, 1790–1793. (b) Brøndsted Nielsen, M. Model Systems for Understanding Absorption Tuning by Opsin Proteins. *Chem. Soc. Rev.* **2009**, *38*, 913–924.
- (4) (a) Navizet, I.; Liu, Y. J.; Ferré, N.; Xiao, H. Y.; Fang, W. H.; Lindh, R. Color-Tuning Mechanism of Firefly Investigated by Multi-Configurational Perturbation Method. *J. Am. Chem. Soc.* **2010**, *132*, 706–712. (b) Cai, D.; Marques, M. A. L.; Milne, B. F.; Nogueira, F. Bioheterojunction Effect on Fluorescence Origin and Efficiency Improvement of Firefly Chromophores. *J. Phys. Chem. Lett.* **2010**, *1*, 2781–2787.
- (5) Reichardt, C. Solvatochromic Dyes as Solvent Polarity Indicators. *Chem. Rev.* **1994**, *94*, 2319–2358.
- (6) Kosower, E. M. The Effect of Solvent on Spectra. I. A New Empirical Measure of Solvent Polarity: Z-Values. *J. Am. Chem. Soc.* **1958**, *80*, 3253–3260.
- (7) Kamlet, M. J.; Abboud, J. L.; Taft, R. W. The solvatochromic comparison method. 6. The  $\pi^*$  scale of solvent polarities. *J. Am. Chem. Soc.* **1977**, *99*, 6027–6038.
- (8) (a) Kamlet, M. J.; Taft, R. W. The solvatochromic comparison method. I. The  $\beta$ -scale of solvent hydrogen-bond acceptor (HBA) basicities. *J. Am. Chem. Soc.* **1976**, *98*, 377–383. (b) Taft, R. W.;



Kamlet, M. J. The solvatochromic comparison method. 2. The  $\alpha$ -scale of solvent hydrogen-bond donor (HBD) acidities. *J. Am. Chem. Soc.* **1976**, *98*, 2886–2894.

(9) Kirketerp, M.-B. S.; Petersen, M. Å.; Wanko, M.; Leal, L. A. E.; Zettergren, H.; Raymo, F. M.; Brøndsted Nielsen, M.; Brøndsted Nielsen, S. Absorption Spectra of 4-Nitrophenolate Ions Measured in Vacuo and in Solution. *ChemPhysChem* **2009**, *10*, 1207–1209.

(10) Kirketerp, M.-B. S.; Petersen, M. Å.; Wanko, M.; Zettergren, H.; Rubio, A.; Brøndsted Nielsen, M.; Brøndsted Nielsen, S. Double-Bond versus Triple-Bond Bridges: Does it Matter for the Charge-Transfer Absorption by Donor-Acceptor Chromophores? *ChemPhysChem* **2010**, *11*, 2495–2498.

(11) Wanko, M.; Houmøller, J.; Stöckel, K.; Kirketerp, M.-B. S.; Petersen, M. Å.; Brøndsted Nielsen, M.; Brøndsted Nielsen, S.; Rubio, A. Substitution effects on the absorption spectra of nitrophenolate isomers. *Phys. Chem. Phys.* **2012**, *14*, 12905–12911.

(12) Houmøller, J.; Wanko, M.; Stöckel, K.; Rubio, A.; Brøndsted Nielsen, S. On the Effect of a Single Solvent Molecule on the Charge-Transfer Band of a Donor-Acceptor Anion. *J. Am. Chem. Soc.* **2013**, *135*, 6818–6821.

(13) Christensen, M. A.; Della Pia, E. A.; Houmøller, J.; Thomsen, S.; Wanko, M.; Bond, A. D.; Rubio, A.; Brøndsted Nielsen, S.; Brøndsted Nielsen, M. Cross-Conjugation versus Linear Conjugation in Donor-Bridge-Acceptor Nitrophenol Chromophores. *Eur. J. Org. Chem.* **2014**, *2014*, 2044–2052.

(14) (a) Kirketerp, M.-B. S.; Leal, L. A. E.; Varsano, D.; Rubio, A.; Jørgensen, T. J. D.; Kilså, K.; Brøndsted Nielsen, M.; Brøndsted Nielsen, S. On the intrinsic optical absorptions by tetrathiafulvalene radical cations and isomers. *Chem. Commun.* **2011**, *47*, 6900–6902. (b) Panja, S.; Kadhane, U.; Andersen, J. U.; Holm, A. I. S.; Hvelplund, P.; Kirketerp, M.-B. S.; Brøndsted Nielsen, S.; Stöckel, K.; Compton, R. N.; Forster, J. S.; Kilså, K.; Brøndsted Nielsen, M. Dianions of 7,7,8,8-tetracyano-*p*-quinodimethane and perfluorinated tetracyanoquinodimethane: Information on excited states from lifetime measurements in an electrostatic storage ring and optical absorption spectroscopy. *J. Chem. Phys.* **2007**, *127*, 124301.

(15) (a) Wyer, J. A.; Brøndsted Nielsen, S. Absorption by Isolated Ferric Heme Nitrosyl Cations in Vacuo. *Angew. Chem., Int. Ed.* **2012**, *51*, 10256–10260. (b) Stöckel, K.; Milne, B. F.; Brøndsted Nielsen, S. Absorption Spectrum of the Firefly Luciferin Anion Isolated in Vacuo. *J. Phys. Chem. A* **2011**, *115*, 2155–2159.

(16) (a) Andersen, J. U.; Hvelplund, P.; Brøndsted Nielsen, S.; Tomita, S.; Wahlgreen, H.; Møller, S. P.; Pedersen, U. V.; Forster, J. S.; Jørgensen, T. J. D. The combination of an electrospray ion source and an electrostatic storage ring for lifetime and spectroscopy experiments on biomolecules. *Rev. Sci. Instrum.* **2002**, *73*, 1284–1287. (b) Stöckel, K.; Kadhane, U.; Andersen, J. U.; Holm, A. I. S.; Hvelplund, P.; Kirketerp, M.-B. S.; Larsen, M. K.; Lykkegaard, M. K.; Brøndsted Nielsen, S.; Panja, S.; Zettergren, H. A new technique for time-resolved daughter ion mass spectrometry on the microsecond to millisecond time scale using an electrostatic ion storage ring. *Rev. Sci. Instrum.* **2008**, *79*, 023107.

(17) Wyer, J. A.; Ehlerding, A.; Zettergren, H.; Kirketerp, M.-B. S.; Brøndsted Nielsen, S. Tagging of Protonated Ala-Tyr and Tyr-Ala by Crown Ether Prevents Direct Hydrogen Loss and Proton Mobility after Photoexcitation: Importance for Gas-Phase Absorption Spectra, Dissociation Lifetimes, and Channels. *J. Phys. Chem. A* **2009**, *113*, 9277–9285.

(18) Rajput, J.; Rahbek, D. B.; Aravind, G.; Andersen, L. H. Spectral Tuning of the Photoactive Yellow Protein Chromophore by H-bonding. *Biophys. J.* **2010**, *98*, 488–492.

(19) (a) Tozer, D. J. Relationship between long-range charge-transfer excitation energy error and integer discontinuity in Kohn-Sham theory. *J. Chem. Phys.* **2003**, *119*, 12697–12699. (b) Dreuw, A.; Weisman, J. L.; Head-Gordon, M. Long-range charge-transfer excited states in time-dependent density functional theory require non-local exchange. *J. Chem. Phys.* **2003**, *119*, 2943–2946.

(20) Nakatsu, T.; Ichiyama, S.; Hiratake, J.; Saldanha, A.; Kobashi, N.; Sakata, K.; Kato, H. Structural basis for the spectral difference in luciferase bioluminescence. *Nature* **2006**, *440*, 372–376.

(21) (a) Hoffmann, M.; Wanko, M.; Strodel, P.; König, P. H.; Frauenheim, T.; Schulten, K.; Thiel, W.; Tajkhorshid, E.; Elstner, M. Color tuning in rhodopsins: The mechanism for the spectral shift between bacteriorhodopsin and sensory rhodopsin II. *J. Am. Chem. Soc.* **2006**, *128*, 10808–10818. (b) Nakatani, N.; Hasegawa, J.; Nakatsuji, H. Red light in chemiluminescence and yellow-green light in bioluminescence: Color-tuning mechanism of firefly, *Photinus pyralis*, studied by the symmetry-adapted cluster-configuration interaction method. *J. Am. Chem. Soc.* **2007**, *129*, 8756–8765. (c) Shu, X. K.; Shaner, N. C.; Yarbrough, C. A.; Tsien, R. Y.; Remington, S. J. Novel chromophores and buried charges control color in mFruits. *Biochemistry* **2006**, *45*, 9639–9647. (d) Nienhaus, G.; Nienhaus, K.; Wiedenmann, J. Structure-Function Relationships in Fluorescent Marker Proteins of the Green Fluorescent Protein Family. *Springer Ser. Fluoresc.* **2012**, *11*, 241–264.

(22) Stöckel, K.; Hansen, C. N.; Houmøller, J.; Nielsen, L. M.; Anggara, K.; Linares, M.; Norman, P.; Nogueira, F.; Maltsev, O. V.; Hintermann, L.; Brøndsted Nielsen, S.; Naumov, P.; Milne, B. F. On the Influence of Water on the Electronic Structure of Firefly Oxyluciferin Anions from Absorption Spectroscopy of Bare and Monohydrated Ions in Vacuo. *J. Am. Chem. Soc.* **2013**, *135*, 6485–6493.

(23) Zuev, D.; Bravaya, K. B.; Makarova, M. V.; Krylov, A. I. Effect of microhydration on the electronic structure of the chromophores of the photoactive yellow and green fluorescent proteins. *J. Chem. Phys.* **2011**, *135*, 194304.

(24) Müllen, K.; Wegner, G., Eds. *Electronic Materials: The Oligomer Approach*; Wiley-VCH: Weinheim, 1998.

(25) Rocha-Rinza, T.; Christiansen, O.; Rahbek, D. B.; Klærke, B.; Andersen, L. H.; Lincke, K.; Brøndsted Nielsen, M. Spectroscopic implications of the electron donor-acceptor effect in the Photoactive Yellow Protein chromophore. *Chem.—Eur. J.* **2010**, *16*, 11977–11984.

(26) (a) Brøndsted Nielsen, M.; Diederich, F. Conjugated Oligoenynes Based on the Diethynylethene Unit. *Chem. Rev.* **2005**, *105*, 1837–1867. (b) Gholami, M.; Tykwinski, R. R. Oligomeric and Polymeric Systems with a Cross-conjugated  $\pi$ -Framework. *Chem. Rev.* **2006**, *106*, 4997–5027. (c) Hopf, H.; Sherburn, M. S. Dendralenes Branch Out: Cross-Conjugated Oligoenes Allow the Rapid Generation of Molecular Complexity. *Angew. Chem., Int. Ed.* **2012**, *51*, 2298–2338.

(27) Ricks, A. B.; Solomon, G. C.; Colvin, M. T.; Scott, A. M.; Chen, K.; Ratner, M. A.; Wasielewski, M. R. Controlling Electron Transfer in Donor-Bridge-Acceptor Molecules Using Cross-Conjugated Bridges. *J. Am. Chem. Soc.* **2010**, *132*, 15427–15434.

(28) (a) Cheng, L. T.; Tam, W.; Marder, S. R.; Stiegman, A. E.; Rikken, G.; Spangler, C. W. Experimental investigations of organic molecular nonlinear optical polarizabilities. 2. A study of conjugation dependences. *J. Phys. Chem.* **1991**, *95*, 10643–10652. (b) Andreu, R.; de Lucas, A. I.; Garin, J.; Martin, N.; Orduna, J.; Sanchez, L.; Seoane, C. New TTF-based donor-acceptor molecules linked by flexible ethylenic spacers. *Synth. Met.* **1997**, *86*, 1817–1818. (c) Andersson, A. S.; Diederich, F.; Brøndsted Nielsen, M. Acetylenic tetrathiafulvalene-dicyanovinyl donor-acceptor chromophores. *Org. Biomol. Chem.* **2009**, *7*, 3474–3480.

(29) (a) Kushmerick, J. G.; Holt, D. B.; Pollack, S. K.; Ratner, M. A.; Yang, J. C.; Schull, T. L.; Naciri, J.; Moore, M. H.; Shashidhar, R. Effect of Bond-Length Alternation in Molecular Wires. *J. Am. Chem. Soc.* **2002**, *124*, 10654–10655. (b) Cai, L. T.; Skulason, H.; Kushmerick, J. G.; Pollack, S. K.; Naciri, J.; Shashidhar, R.; Allara, D. L.; Mallouk, T. E.; Mayer, T. S. Nanowire-Based Molecular Monolayer Junctions: Synthesis, Assembly, and Electrical Characterization. *J. Phys. Chem. B* **2004**, *108*, 2827–2832. (c) Huber, R.; González, M. T.; Wu, S.; Langer, M.; Grunder, S.; Horhoiu, V.; Mayor, M.; Bryce, M. R.; Wang, C. S.; Jitchati, R.; Schönenberger, C.; Calame, M. Electrical Conductance of Conjugated Oligomers at the Single Molecule Level. *J. Am. Chem. Soc.* **2008**, *130*, 1080–1084.



(30) (a) Mayor, M.; Weber, H. B.; Reichert, J.; Elbing, M.; von Hänisch, C.; Beckmann, D.; Fischer, M. Electric Current through a Molecular Rod—Relevance of the Position of the Anchor Groups. *Angew. Chem., Int. Ed.* **2003**, *42*, 5834–5838. (b) Solomon, G. C.; Andrews, D. Q.; Van Duyne, R. P.; Ratner, M. A. When Things Are Not as They Seem: Quantum Interference Turns Molecular Electron Transfer “Rules” Upside Down. *J. Am. Chem. Soc.* **2008**, *130*, 7788–7789. (c) Kronemeijer, A. J.; Akkerman, H. B.; Kudernac, T.; van Wees, B. J.; Feringa, B. L.; Blom, P.; de Boer, B. Reversible Conductance Switching in Molecular Devices. *Adv. Mater.* **2008**, *20*, 1467–1473. (d) van der Molen, J. S.; Liao, J.; Kudernac, T.; Agustsson, J. S.; Bernard, L.; Calame, M.; van Wees, B. J.; Feringa, B. L.; Schönenberger, C. Light-Controlled Conductance Switching of Ordered Metal–Molecule–Metal Devices. *Nano Lett.* **2009**, *9*, 76–80. (e) Fock, J.; Leijnse, M.; Jennum, K.; Zyazin, A. S.; Paaske, J.; Hedegård, P.; Brøndsted Nielsen, M.; van der Zant, H. S. J. Manipulation of organic polyradicals in a single-molecule transistor. *Phys. Rev. B* **2013**, *86*, 235403.